Applied Catalysis A: General 355 (2009) 20–26

Contents lists available at ScienceDirect

Applied Catalysis A: General

journal homepage: www.elsevier.com/locate/apcata

A new activation process of bimetallic catalysts and application to the *n*-hexane isomerization

Carlos M.N. Yoshioka [a], Maura H. Jordão [b,1], Daniela Zanchet [b], Teresita F. Garetto [c], Dilson Cardoso [a,*]

[a] Federal University of São Carlos, Chemical Engineering Department, Catalysis Laboratory (LabCat), P.O. Box 676, 13560 São Carlos – SP, Brazil
[b] Brazilian Synchrotron Light Laboratory (LNLS), P.O. Box 6192, Campinas – SP, Brazil
[c] Instituto de Investigaciones en Catálisis y Petroquímica (FIQ–CONICET-UNL), 3000 Santa Fe, Argentina

ARTICLE INFO

Article history:
Received 13 July 2008
Received in revised form 27 October 2008
Accepted 28 October 2008
Available online 5 November 2008

Keywords:
Bimetallic catalyst
Fast activation
n-Hexane isomerization
XANES
TEM

ABSTRACT

Bimetallic catalysts applied to the *n*-hexane isomerization reaction were prepared with a constant molar content of 130 μmol Me/g_{cat} of Ni and Pt and characterized in its active form by X-ray absorption near edge spectroscopy (XANES), transmission electron microscopy (TEM), temperature programmed reduction and hydrogen chemisorption techniques. The metal was dispersed in a HUSY zeolite matrix in order to provide both types of sites, metallic and acid, to obtain a bifunctional catalyst. The catalytic activity was evaluated using the catalyst activated at different temperatures following a new activation process, named "fast activation method" and the profile pointed out a maximum catalytic activity when the catalyst was activated at 400 °C. XANES results showed that all samples present similar electronic properties in the studied conditions, despite the differences found in the average particle diameter obtained by TEM, suggesting that the catalytic activity is related to the metal/acid balance.

1. Introduction

Environmental concerns have prompted legislation to limit the amount of aromatics in gasoline. However, reduction of aromatics has a negative impact on gasoline octane number that has to be compensated by other means. In view of the paraffin is environmentally more acceptable than aromatics, and the branched paraffin has higher octane numbers than linear alkanes, its use is an attractive alternative to other technologies, such as blending with oxygenates [1,2]. Consequently, an interesting option would be increasing the content of high-octane branched paraffin in the gasoline, which can be achieved through the isomerization of the corresponding linear paraffin [3].

The catalysts normally used in such reaction are bifunctional, comprising a combination of acid and metallic (dehydrogenation/hydrogenation) functions. Usually, they contain noble metals like platinum supported on chlorided alumina. However, these alumina-based catalysts contain volatile chlorides in order to create Brønsted acidity that causes corrosion and pollution problems; moreover, these catalysts are more sensitive to poisons such as sulfur [4–7].

The acidity of bifunctional catalysts can also be provided by zeolites [8], which have an important role in petroleum refining and are applied in processes such as hydrocracking, isomerization and dewaxing [8]. According to the classical bifunctional mechanism proposed by Weisz and Prater [9], the isomerization of alkanes occurs in three consecutive steps: dehydrogenation, isomerization and hydrogenation. The metal phase dehydrogenates the alkanes into alkenes, which are protonated on the Brønsted acid sites yielding carbenium ions. After rearrangement, these carbenium ions desorb from the acid sites as alkenes and are hydrogenated at the metal phase yielding saturated reaction products [10].

The interest in bimetallic heterogeneous catalysts has been increasing since the presence of a second metal can influence the catalytic properties, improving their activity, stability and selectivity [11]. In addition, the reduction properties as well as a higher dispersion can be favored [12]. In some cases, the second metal also increases the resistance to coke poisoning [13].

Bimetallic catalysts composed by Ni and Pt were studied in the isomerization reaction of linear alkanes and interesting results were obtained [11]; since then, many studies have been performed using different metal contents and using different kinds of zeolites as HUSY and BEA [10,11,14–16] types. The usual method of reduction of transition cations in these studies, named "traditional activation", uses several isothermal steps and low heating rates, with a total time reduction of 10 h [8]. Due to the long time

* Corresponding author. Tel.: +55 16 33518264; fax: +55 16 33518266.
E-mail address: dilson@ufscar.br (D. Cardoso).
[1] Now at "Rhodia Poliamida e Especialidades", Paulínia – SP, Brazil.

0926-860X/$ – see front matter © 2008 Elsevier B.V. All rights reserved.
doi:10.1016/j.apcata.2008.10.038

duration of this reduction method, unfavorable processes can occur like the migration of the transition metal cation to the zeolite cavities and the metal particles sintering.

To minimize these problems, the heating rate as well the final temperature in the reduction step was changed, in order to verify their influence in the properties of the catalysts. As result, a new reduction method, called "fast activation" [17] was developed and is detailed in this work. In this way, catalysts containing Pt and Ni as metal sites were supported on a FAU structure and tested in the isomerization of *n*-hexane reaction. The catalysts were characterized by X-ray absorption near edge spectroscopy (XANES), transmission electron microscopy (TEM), temperature programmed reduction (TPR) and hydrogen chemisorption techniques.

2. Experimental

2.1. Catalyst preparation

A bimetallic catalyst containing a constant molar content of the 130 μmol Me/g_{cat}, with a 50–50 proportion of Pt–Ni was prepared using the $Ni(NH_3)_6Cl_2$ and $Pt(NH_3)_4Cl_2$ as metals precursors and a competitive ion exchange method [16]. A monometallic platinum catalyst with the same molar content was also prepared, for comparison. A HUSY zeolite, granted by Engelhard (EZ-190P), was chosen, with a framework Si/Al ratio equal 11, confirmed by X-ray diffraction. To obtain better ion exchange efficiency with the transitions metals, the initial zeolite was converted to its ammonium form [15–17].

The aqueous solution of the metallic precursors containing NH_4Cl was added gradually to the zeolite suspension in water, stirring for 1 h at 25 °C and then filtered, washed and dried at 110 °C for 2 h. The chemical composition of the solid was estimated by analysis of the filtrate by inductively coupled plasma spectroscopy (ICP) and, for these samples, the exchange efficiency was approximately 100%.

2.2. Catalyst activation

The calcination step was carried out heating the materials at 2 °C min^{-1} to 500 °C under 100 mL min^{-1} g^{-1} of solid of synthetic air flow and kept at this temperature for 2 h to eliminate ammonia from the ammonium-form zeolite and from the transition metal complexes used. To obtain the active catalysts, the samples were reduced under pure hydrogen flow at a specific temperature and time. In the "*traditional activation*" method [15], the temperature was ramped at 2 °C min^{-1} up to 500 °C and kept for 6 h under 100 mL min^{-1} g^{-1} hydrogen flow; in the "*fast activation*" method [17], a faster ramp was used, 30 °C min^{-1}, and the samples were heated to a specific temperature and kept for 30 min. The set points used were 350, 400, 450, 500 and 550 °C. For comparison, two catalysts were prepared by the *traditional activation* method, at 450 and 500 °C temperatures. The samples description is shown in Table 1, and were labeled as *X*Pt*Θ*A, where:

*X*Pt = *X* indicates the percentage of platinum in the bimetallic Pt–Ni catalyst,
*Θ*A = *Θ* indicates the final reduction temperature and A indicates reduction method,
A = F indicates fast reduction method; A = T indicates traditional method of reduction.

X-ray diffraction of the reduced samples shows no decrease in the peaks intensity, indicating that the zeolite structure was maintained.

Table 1
Identification of the catalysts, containing 130 μmol Me/g catalyst.

Sample	*Θ*, Final activation temperature (°C)	A, Activation method
50Pt350F	350	Fast
50Pt400F	400	Fast
50Pt450F	450	Fast
50Pt450T	450	Traditional
100Pt450F	450	Fast
50Pt500F	500	Fast
50Pt500T	500	Traditional
50Pt550F	550	Fast

2.3. Analysis by temperature programmed reduction

Temperature programmed reduction analyses were done to obtain the correlation between the final reduction temperature in the fast activation process and the reduction grade of the transition metal cations. The equipment used was a Micromeritics (ChemiSorb 2705) equipped with a thermal conductivity detector (TCD). Before the TPR measurement, the samples were activated *in situ*, following the fast activation process previously described, at final temperatures of 400, 450 and 500 °C. Then, the TPR measurement was initiated using a carrier gas of 5%H_2/N_2. The reactor was heated up to 1000 °C at a constant rate of 10 °C min^{-1} and the water product was trapped by a cold trap (ethanol plus liquid nitrogen).

2.4. Transmission electron microscopy and X-ray energy dispersive spectroscopy

Transmission electron microscopy investigation was done for the 50Pt350F, 50Pt450F, 50Pt500F and 50Pt500T catalysts. The samples were prepared by dispersing the powder ultrasonically in isopropyl alcohol and dropping this suspension on an amorphous carbon coated copper grid. A high resolution transmission electron microscope (HR-TEM JEM 3010 URP) at LME-LNLS, Campinas, Brazil, operating at 300 kV with a point resolution of 0.17 nm was used. X-ray energy dispersive spectroscopy (EDS) analyses (Noram Voyager) were performed using probes of 10–25 nm.

2.5. X-ray absorption near-edge structure

X-ray absorption near-edge structure measurements were carried out at the D04B-XAFS1 beamline of the LNLS – Campinas, Brazil, using a Si (1 1 1) channel-cut crystal monochromator. The spectra of platinum L_2 (E_0 = 13.273 keV) and L_3 (E_0 = 11.564 keV) edges were obtained in transmission mode. The activated powder catalysts were placed in acrylic sample holders and sealed by Kapton tape inside a dry box. The reference material was the platinum foil, which was also used for the monochromator calibration.

To quantify the differences between the white line intensities of $L_{2,3}$-edges, the method described by Mansour et al. [18] was applied taking in account the same considerations to make valid comparison between spectra: subtraction of the pre-edge background from the entire range of the data to remove the contribution of all other electrons to the XANES spectrum; L_2 absorption edge was aligned by adjusting the energy scale to align the extended X-ray absorption fine structure (EXAFS) oscillations in both edges; the spectra normalization was done at the point where the oscillations were aligned.

After plotting reference and sample data spectra, the difference spectrum was obtained and the resulting curve was integrated between 10 eV to +14 eV at both L_2-edge and L_3-edge to get the ΔA_2 and ΔA_3, respectively. Following the Mansour et al. [18] work, the

fractional change in the total number of d-band unoccupied states of the sample compared to that of platinum foil, f_d was defined as

$$f_d = \frac{\Delta A_3 \times \sigma_3 + 1.11 \times \Delta A_2 \times \sigma_2}{A_{3r} \times \sigma_3 + 1.11 \times A_{2r} \times \sigma_2} \quad (1)$$

The areas were normalized by multiplying by the platinum density (ρ) and absorption cross-section (σ), where $\sigma_2 = \sigma L_2(54.2\ cm^2/g) \times \rho(21.37)$ and $\sigma_3 = \sigma L_3(117.1\ cm^2/g) \times \rho(21.37)$. The term $(A_{3r} \times \sigma_3 + 1.11 \times A_{2r} \times \sigma_2 = 1.92 \times 10^4)$ was calculated. From the fractional number calculated using Eq. (1), it was possible to calculate the number of unoccupied 5d states of the Pt in the bimetallic sample, h_{TS}, defined as

$$h_{TS} = \frac{(1 + f_d)}{h_{TR}} \quad (2)$$

For platinum (reference), the number of unoccupied 5d states (h_{TR}) was assumed to be 0.30 [18].

2.6. Analysis by hydrogen chemisorption

Volumetric adsorption experiments were performed at 298 K in a conventional vacuum unit. The pre-treatments to activate the samples were the same as done for the TPR analyses, and then, the samples were outgassed 2 h at 773 K prior performing gas chemisorption experiments. Hydrogen uptake was determined using the double isotherm method. After cooling to room temperature a first isotherm (primary isotherm) was drawn for measuring the total hydrogen uptake. Then, and after 1 h of evacuation at room temperature, a second isotherm (secondary isotherm) was performed to determine the amount of weakly adsorbed hydrogen. The amount of irreversibly chemical adsorbed hydrogen, $(HC)_i$ was calculated as the difference between total and weakly adsorbed hydrogen. The pressure range of isotherms was 0–6.6 kPa.

2.7. Catalytic tests

The reaction used to test the catalysts was the *n*-hexane isomerization and it was performed at 250 °C under atmospheric pressure, maintaining a molar ratio of 9:1 (H_2:*n*-C_6H_{14}); the catalysts were activated *in situ* in a fixed bed reactor and the reaction products were analyzed on-line using a gas chromatograph (Varian Star 3400) using a flame ionization detector and a capillary column (CB-1). The reactor contained a known mass of catalyst (about 0.1 g) and was fed with *n*-hexane under a 2 mL h^{-1} flow, resulting a W/F contact time of about 0.076 h.

3. Results and discussion

3.1. Characterization by temperature programmed reduction

Fig. 1 shows the TPR profiles of the original catalyst precursor and some of the samples submitted to the fast activation method, as described in Table 1. The attribution of the reduced species to each peak of the TPR profile in these samples can be done considering the results of Jordão et al. [15] that studied monometallic Pt^{2+}/HUSY and Ni^{2+}/HUSY samples. Three peaks are expected in the TPR profiles of monometallic samples, representing the reduction of cations located at supercage (α), sodalite cage (β) and hexagonal prisms (γ) of FAU zeolite structure. Depending on where the cations are located, the reduction of these monometallic samples occurs between 200 and 450 °C in the case of Pt^{2+}/HUSY and between 500 and 800 °C in the case of Ni^{2+}/HUSY. However, when Ni is combined with another transition metal, its reduction temperature can be decreased; for this particular system (Pt–Ni dispersed in a HUSY matrix), the Ni^{2+} reduction temperature decreases approximately 60 °C depend on Pt content [15,19].

In the TPR of the original catalyst precursor (Fig. 1a), it can be seen at least three peaks of reduction, the first one corresponds to Pt^{2+} in the sodalite cage (β_{Pt}), the second one is a superposition of Ni^{2+} present in the supercage (α_{Ni}) and Pt^{2+} in the hexagonal prisms (γ_{Pt}) and the last one corresponds to the Ni^{2+} present in the sodalite cage (β_{Ni}).

The TPR profile of those samples submitted previously to "fast activation method", at different final temperatures, are shown in curves (b)–(d) of Fig. 1. Fig. 1 also shows the percentage of not reduced Pt and Ni cations, compared to the TPR area of the original sample (a). It can be observed that, as a consequence of the short reduction period of this method, there are unreduced species for all activated samples and that the amount of remaining unreduced cations decreases as the final reduction temperature increases.

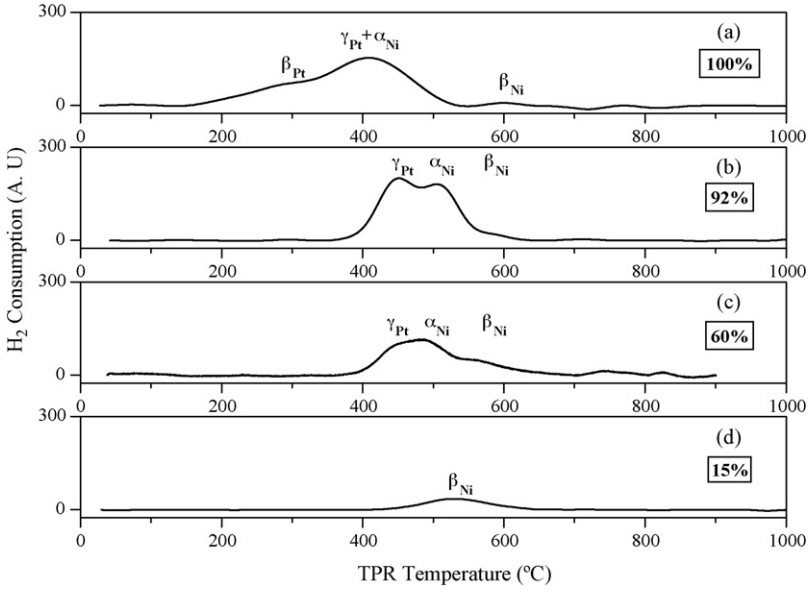

Fig. 1. TPR profiles of the (a) 50Pt original (not activated), (b) 50Pt400F, (c) 50Pt450F and (d) 50Pt500F samples.

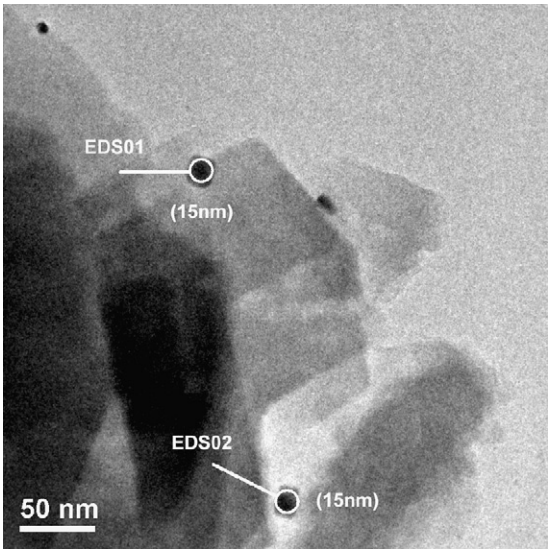

Fig. 2. TEM and EDS of bimetallic catalyst, reduced by the fast activation method, at temperature of 350 °C (50Pt350F).

The TPR performed after the activation process, at all final temperatures (Fig. 1b–d), shows the disappearance of the first peak, attributed to Pt^{2+} located in the sodalite cages (β). The Pt^{2+} ions located at the hexagonal prisms (γ) are totally reduced only when the sample is pre-activated at 500 °C. The remained reduction peak at temperatures about 500° was attributed to the reduction of the Ni^{2+} cations located in great cavity (α) and the small peak at about 600 °C, to the sodalite cage (β), which agrees with the difficulty of the reduction in the less accessible positions of the FAU structure.

3.2. Transmission electron microscopy and X-ray energy dispersive spectroscopy

TEM images and EDS spectra of the bimetallic samples are shown in Figs. 2–4. It is possible to observe in all images the presence of metal particles dispersed on the zeolite matrix (see for example the white arrows in Fig. 4). From EDS analysis of some large particles, only platinum was identified, suggesting that the majority of these large metallic particles are composed by this metal (see Figs. 2 and 3). Consequently, as verified by TPR (Fig. 1b–d) most of the nickel is probably dispersed in the matrix in the cationic form, compensating the anionic sites of the zeolite. The signal of Si, Al and Cu elements come from the zeolite matrix and the copper grid.

The average dimensions of the metallic particles as a function of the activation temperature were estimated from the analysis of 30–50 particles. The results are presented in Table 2, which shows that the average particle diameter of the samples reduced by the fast activation method was in the range of 2.6–6.9 nm. Despite the low statistics, it is possible to verify that the average particle diameter decreases when the temperature of activation increases from 350 to 450 °C. This Table also shows that the average diameter of the catalyst reduced by the "traditional activation method" (50Pt500T) is much higher, as a consequence of sinterization of the metallic particles, submitted at high temperatures for long periods of time.

3.3. Analysis by X-ray absorption spectroscopy

Fig. 5 presents L_2 and L_3 edges absorption edges spectra for platinum foil. The L_2 absorption edge was aligned by adjusting the energy scale to align the EXAFS oscillation in both edges (from $E - E_0 = 45$ eV) as suggest by Mansour et al. [18].

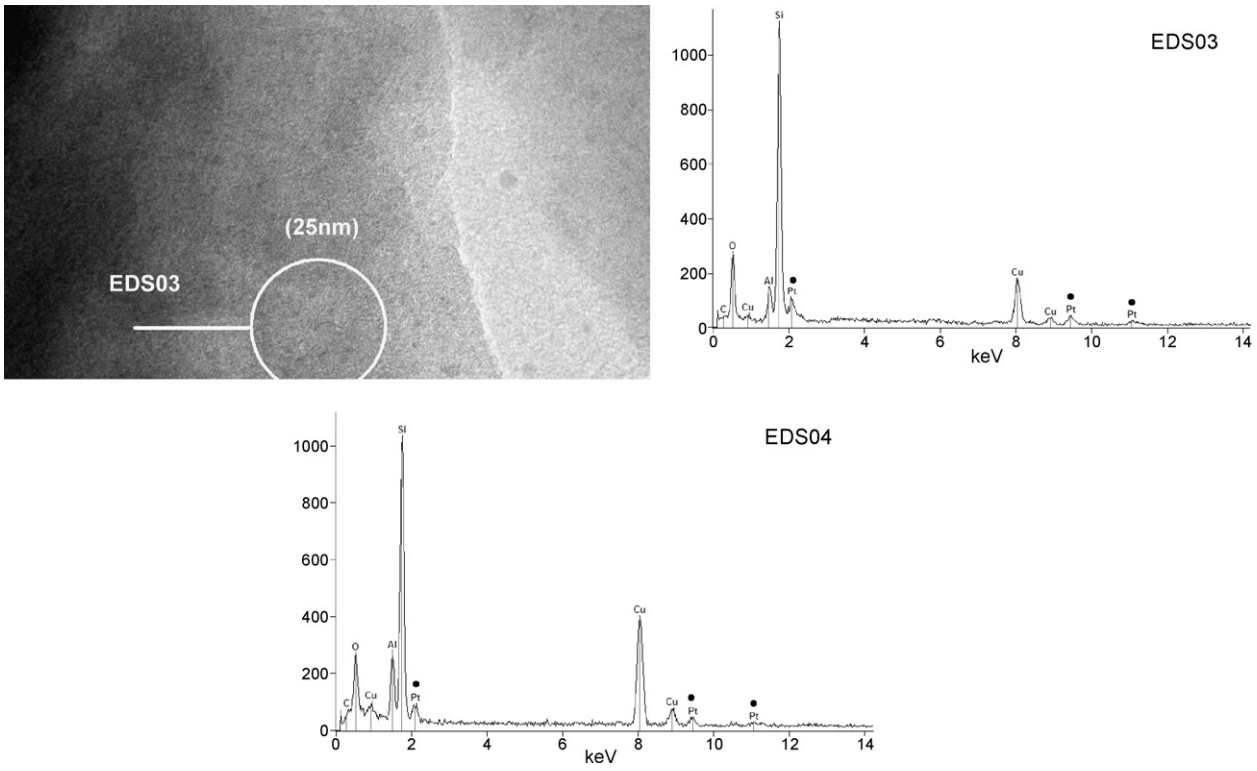

Fig. 3. TEM and EDS of bimetallic catalyst reduced by the fast activation method, at temperature of 450 °C (50Pt450F).

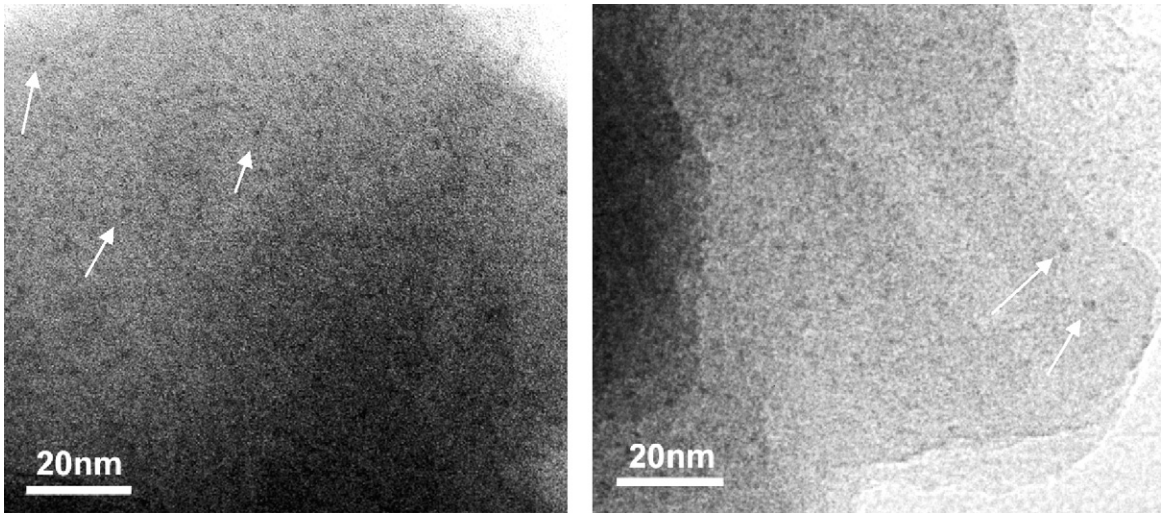

Fig. 4. TEM of bimetallic catalyst reduced by the fast activation method, at temperature of 500 °C (50Pt500F). The white arrows indicate Pt nanoparticles.

As shown in Fig. 5, the spin–orbit interaction in both core and valence levels [20] introduce clear differences between the white lines (shape and intensity) at both edges. For a particular kind of metal, any dissimilarity of the density of unoccupied sites above Fermi level will be showed by the intensity of the white line [21], and this characteristic can be used to detect electronic density changes in multimetallic catalysts and adsorbate interactions. In general, the electronic configuration of d-band of the metal can be related to the catalytic activity [22] and this feature can be monitored by the white line study using the L-edges of the element.

The reason to explore Pt $L_{2,3}$-edges is because XANES spectra will provide information about the unoccupied states density near Fermi level using the white line as a probe. The L_3 white line probes the transition from $2p_{3/2}$ initial state to $5d_{5/2}$ and $5d_{3/2}$ final states, while the L_2 white line probes the transition from $2p_{1/2}$ initial state to $5d_{3/2}$ final state according to dipole selection rules [23]. Due to the spin–orbit effect, the unoccupied d-state in an isolated Pt atom is the $5d_{5/2}$ and besides the broadening inside the band in a Pt bulk, the d-band vacancies near Fermi level have predominate $5d_{5/2}$ character. Therefore, if it is possible to probe the final states separately, any effect on the d-band occupation would give important information.

Table 2
Average size of metallic particles obtained at different conditions of activation.

Temperature (°C)	Average diameter (nm)
50Pt350F	6.9
50Pt450F	2.6
50Pt500F	3.3
50Pt500T	15.9

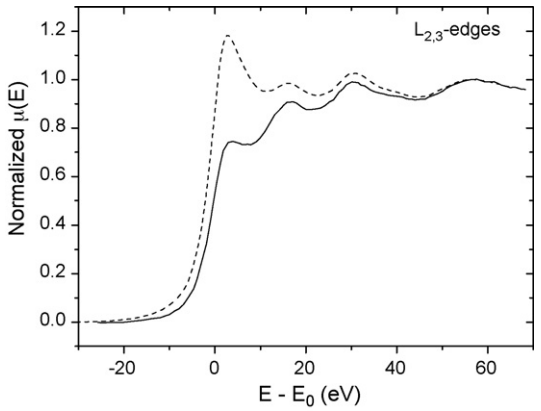

Fig. 5. Normalized L_2 (solid) L_3 (dash) absorption edges of Pt foil reference.

Normalized L_2 and L_3 absorption edges and the difference spectra were done for the 50Pt350F, 50Pt450F, 100Pt450F and 50Pt500T samples. Fig. 6 illustrates the results for the sample 50Pt350F.

The L_2 and L_3 difference spectra contain for all samples a positive peak near the edge showing that this feature is present in spectra samples but absent in the reference. Consequently, if the white line is more intense in the samples spectra, there are higher densities of unoccupied d-states for the samples compared to Pt foil. In addition, because of the presence of this peak in both edges it is feasible to affirm that the electronic vacancies are taking place on the $5d_{5/2}$ and $5d_{3/2}$ final states.

The fractional change in the total number of d-band unoccupied states of the sample compared to the number in platinum foil (f_d) and the number of unoccupied 5d states (h_{TS}) were calculated according to equations described in the experimental section and are summarized in Table 3.

The results show that the change in the number of unoccupied 5d states for all catalysts is not significant; despite the Ni presence in the bimetallic catalysts and the difference in the average particle size obtained by TEM. However, when the catalysts are compared to the platinum foil, an electronic deficiency of the platinum present at all catalysts was identified. Ramallo-López and collaborators also did not observe a significant variation of the d-band electrons density for particles size between 28 and 49 Å [24].

Previous works on Pt supported in inert matrix have shown that a metal–support interaction was not considerable for these

Table 3
$L_{2,3}$ edges areas, fractional change in the number of d-band vacancies relative to the reference material (f_d) and total number of unoccupied d states (h_{TS}).

Sample	ΔA_2 (eV)	ΔA_3 (eV)	f_d[a]	h_{TS}[a]
100Pt450F	1.34	1.80	0.29	0.39
50Pt350F	2.15	2.79	0.47	0.44
50Pt450F	2.31	2.12	0.44	0.43
50Pt500T	1.30	2.42	0.33	0.40

[a] Error = ± 0.02.

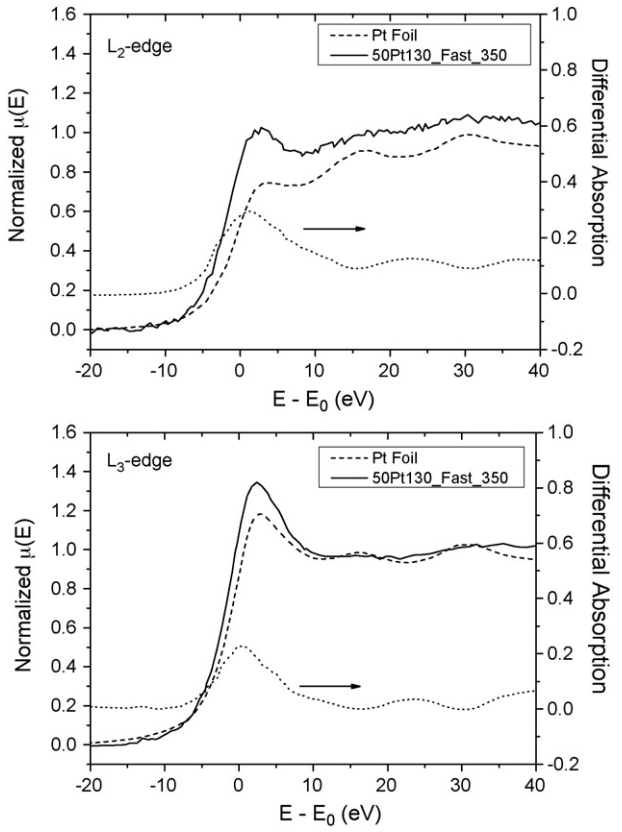

Fig. 6. Normalized L_2 and L_3 Pt-edges XANES spectra for the 50Pt350F sample (solid), Pt foil (dash) reference and the difference spectra (dot).

systems, once there was no difference between Pt foil and catalysts spectra [25,26]. Nevertheless, it has been showed that platinum in supports that present acid properties, an electronic deficiency is identified and many authors relate this effect to the electron-support transference [27–29]. In our work, the support used is a zeolite in a protonic form and it is reasonable to infer that the electronic deficiency observed by XANES in these experiments is caused by an interaction between metal and support, probably through the metal–proton adduct formation [30–32].

3.4. Analysis of the catalysts by hydrogen chemisorption

Fig. 7 shows the quantity of the hydrogen chemisorbed [μmol H_2/g_{cat}] as a function of the activation temperature of the catalyst. These materials were obtained from a fast activation and 30 min at the reduction temperature.

Considering that the results from hydrogen chemisorption represent the number of moles required to form a complete monolayer of hydrogen on the metal surface, the information obtained from this analysis is proportional to the number of surface metal atoms. Therefore, the increase in the activation temperature leads to an increase in the number of surface metal atoms, reaching a maximum at 450 °C and a decrease at higher temperatures. This behavior is in agreement with the trend in the average metal particles size, as shown in Table 2. It is important to point out also that the catalysts reduced below 500 °C have a high proportion of unreduced metal cations, as showed by TPR analyses (Fig. 1). Consequently, the increase of hydrogen chemisorption is not related only to the dimensions of the metal particles, but also to an increase of the number of metal particles, as a consequence of a higher reduction degree of the corresponding cations.

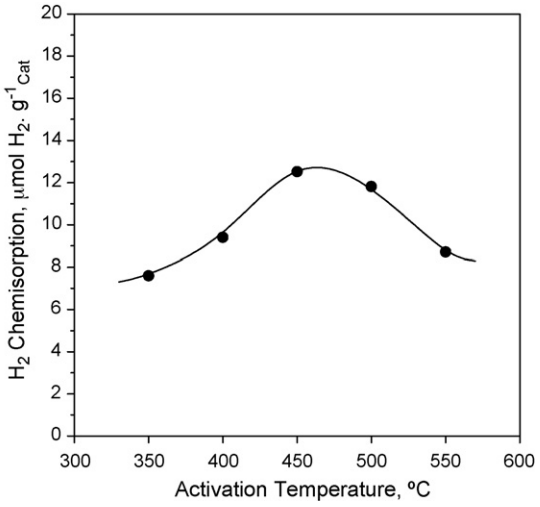

Fig. 7. Hydrogen chemisorption as a function of activation temperature for the bimetallic catalysts, reduced by the fast activation method.

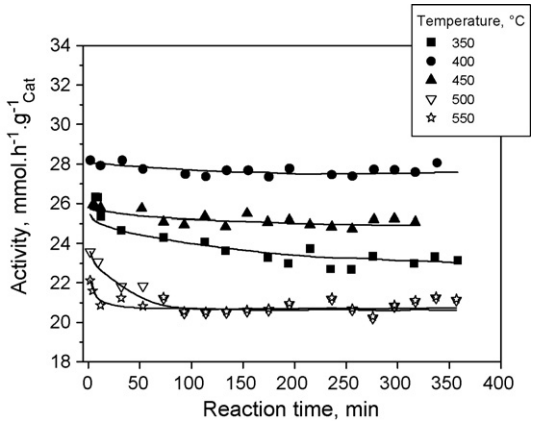

Fig. 8. Activity of the bimetallic catalysts at 250 °C, as a function of time on stream, reduced by the "fast activation method" at different activation temperatures.

3.5. Catalytic isomerization of n-hexane

Fig. 8 presents the catalytic activity of *n*-hexane isomerization as a function of reaction time. Curiously, the catalysts prepared at intermediate temperatures (400–450 °C) are catalytically more stable, which was not expected considering that they have high amounts of unreduced transition cations (see Fig. 1). In order to obtain the properties of the catalyst with no deactivation, the activities as a function of the reaction time were extrapolated to time equal to zero, obtaining in this way the initial isomerization activity (A_0), as presented in Fig. 9. The initial catalytic activity was obtained adjusting a second order exponential decay function, which, as shown in Fig. 8, gave a good correlation with the experimental points ($r^2 > 0.97$).

The results of the initial activity A_0, as a function of the reduction temperature, using the "fast activation method" are presented in Fig. 9 showing that A_0 (▲) pass through a maximum at 400 °C. Two catalysts using the traditional activation method reduced at 450 and 500 °C were evaluated for comparison. It can be observed that the initial activities of these two catalysts (☆) are comparable to the catalysts activated using the fast method, at these same final temperatures. These results pointed out a very interesting point in as much as to get the same catalytic activity for this bimetallic system, it is necessary only few minutes of

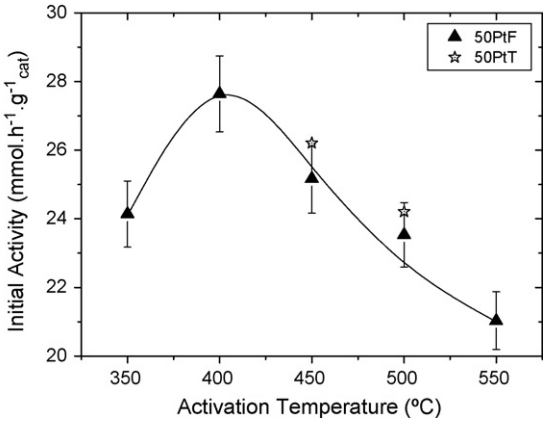

Fig. 9. Initial activity (A_0) of bimetallic catalysts using the fast and traditional activation method, as a function of the reduction temperature.

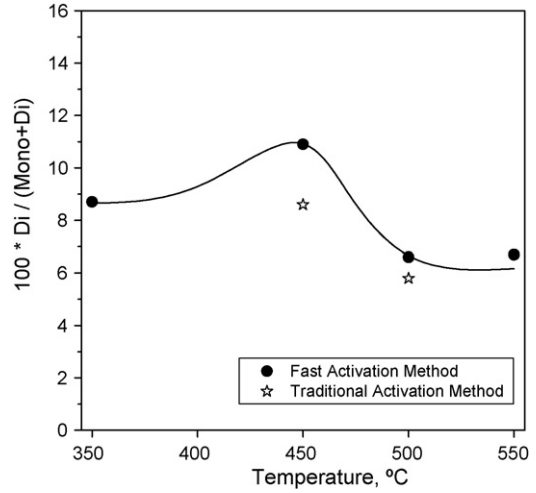

Fig. 10. Selectivity to dibranched hexane isomers as a function of reduction temperature and method.

activation. The total time for the fast activation method is about 30 min, while for the "traditional method" is around 7 h.

It is also interesting to observe that the initial activity A_0 of the catalysts using the fast method reaches its maximum at 400 °C, decreasing with higher reduction temperatures. Comparing these results with the obtained by hydrogen chemisorption (Fig. 7), the maximum initial activity at 400 °C does not coincide exactly with the maximum of the hydrogen chemisorption, which occurs at 450 °C (Fig. 7). This suggests that the catalytic activity is related to the metal/acid balance and not only to the metal dispersion, considering that there are unreduced species even at 500 °C reduction temperature.

Fig. 10 shows that the selectivity to dibranched hexane isomers is not significantly influenced by the final reduction temperature or reduction method (fast activation or traditional).

4. Conclusions

The "fast activation method" of bimetallic precursors containing Pt and Ni metals showed to be a very attractive process for preparing catalysts used in *n*-hexane isomerization, reducing drastically the necessary time to prepare the catalysts, without loss in activity or selectivity to branched isomers.

The TPR analysis performed after the fast activation process indicates that all Pt^{2+} cations present in great cage (α_{Pt}) were reduced at 400 °C and Ni^{2+} cations present in great cage (α_{Ni}) were completely reduced only at 500 °C.

The decrease of the average diameter of the particles measurement by TEM for the catalyst reduced by the fast activation method at 450 °C (50Pt450F) is in good agreement with the maximum hydrogen chemisorption presented by the same catalyst. The maximum catalytic activity at lower temperature (400 °C) suggests that the catalytic activity can be related with the metal/acid balance.

Despite the differences on the average particle size obtained by TEM and the degree of reduction of Ni cations, it was observed no significant change in the catalytic activity and variation in the number of unoccupied 5d states by XANES. Therefore, it can be suggested that the observed electronic deficiency in the samples is not a consequence of a change interaction between Pt and Ni during the different activation methods, but a consequence of an interaction metal–support, probably through Brønsted acid sites.

Acknowledgements

We acknowledge the National Council for Scientific and Technological Development (CNPq) for the scholarship, PRONEX program for the financial support, LME-LNLS for the TEM/EDS measurements and LNLS (Campinas - SP, Brazil) support for the XANES experiments at the D04B-XAFS1 beamline.

References

[1] R. Roldán, F.J. Romero, C. Jiménez-Sanchidrián, J.M. Marinas, J.P. Gómez, Appl. Catal. A: Gen. 288 (2005) 104.
[2] S. Gopal, P.G. Smirniotis, J. Catal. 225 (2004) 278.
[3] M.A. Arribas, F. Márquez, A. Martínez, J. Catal. 190 (2000) 309.
[4] C. Travers, N. Essayem, M. Delage, S. Quelen, Catal. Today 65 (2001) 355.
[5] I. Coleto, R. Roldán, C. Jiménez-Sanchidrián, J.P. Gómez, F.J. Romero-Salguero, Fuel 86 (2007 1000).
[6] H. Liu, G.D. Lei, W.M.H. Sachtler, Appl. Catal. A: Gen. 137 (1996) 167.
[7] A. Chica, A. Corma, J. Catal. 187 (1999) 167.
[8] W.M.H. Sachtler, Z. Zhang, Adv. Catal. 39 (1993) 129.
[9] J.A. Van de Runstraat, P.J. Kamp, J. Stobbelaar, S. van Grondelle, R.A. Krijnen, van Santen, J. Catal. 171 (1997) 77.
[10] E. Blomsma, J.A. Martens, P.A. Jacobs, J. Catal. 165 (1997) 241.
[11] I. Eswaramoorthi, N. Lingappan, Appl. Catal. A: Gen. 245 (2003) 119.
[12] J. Xiao, R.J. Puddephatt, Coordin. Chem. Rev. 143 (1995) 457.
[13] G. Riahi, D. Guillemot, M. Polisset-Thfoin, A.A. Khodadadi, J. Fraissard, Catal. Today 72 (2002) 115.
[14] M.A. Arribas, P. Concepción, A. Martínez, Appl. Catal. A: Gen. 267 (2004) 111.
[15] M.H. Jordão, V. Simões, D. Cardoso, Appl. Catal. A: Gen. 319 (2007) 1.
[16] C.M.N. Yoshioka, T. Garetto, D. Cardoso, Catal. Today 693 (2005) 107.
[17] D. Cardoso, C.M.N. Yoshioka, M.H. Jordão, Patent PI 0603515-9, 2006.
[18] A.N. Mansour, J.W. Cook, D.E. Sayers, R.J. Emrich, J.R. Katzer, J. Catal. 89 (1984) 462.
[19] B. Pawelec, S. Damyanova, K. Arishtirova, J.L.G. Fierro, L. Petrov, Appl. Catal. A: Gen. 323 (2007) 188.
[20] D.E. Ramaker, B.L. Mojet, M.T.G. Oostenbrink, J.T. Miller, D.C. Koningsberger, Phys. Chem. Chem. Phys. 1 (1999) 2293.
[21] Y. Iwasawa (Ed.), X-Ray Absorption Fine Structure for Catalysts and Surfaces, Series on Synchrotron Radiation Techniques and Applications 2, World Scientific Publishing, Singapore, 1996.
[22] J.C.J. Bart, Adv. Catal. 34 (1986) 261.
[23] S.N. Reifsnyder, M.M. Otten, D.E. Sayers, H.H. Lamb, J. Phys. Chem. B 101 (1997) 4972.
[24] J.M. Ramallo-López, F.G. Requejo, A.F. Craievich, J. Wei, M. Avalos-Borja, E. Iglesia, J. Mol. Catal. A: Chem. 228 (2005) 299.
[25] J.H. Sinfelt, G.D. Meitzner, Acc. Chem. Res. 26 (1) (1993) 1.
[26] J.M. Ramallo-López, G.F. Santori, L. Giovanetti, M.L. Casella, O.A. Ferretti, F.G. Requejo, J. Phys. Chem. B 107 (2003) 11441.
[27] R.A. Dalla Betta, M. Boudart, in: Proceedings of the 5th International Congress on Catalysis, North-Holland; New York, 2, (1972), p. 1329.
[28] P. Gallezot, R. Weber, R.A. Dalla Betta, M.Z. Boudart, Naturforsch 34A (1979) 40.
[29] A. Mallmann, D. Barthoumeuf, J. Chem. Phys. 87 (1990) 535.
[30] A. Yu Stakheev, L.M. Kustov, Appl. Catal. A: Gen. 188 (1999) 3.
[31] T.J. McCarthy, G.-D. Lei, W.M.H. Sachtler, J. Catal. 159 (1996) 90.
[32] T.T.T. Wong, W.M.H. Sachtler, J. Catal. 141 (1993) 407.